2018 Building Performance Analysis Conference and
SimBuild co-organized by ASHRAE and IBPSA-USA
Chicago, IL
September 26-28, 2018

A TEST CELL TO INFER THERMAL RESPONSE OF BUILDING COMPONENTS FOR MODEL PREDICTIVE CONTROL USING BUILDING AUTOMATION SENSORS

Elizabeth LeRiche[1], J.J. McArthur[1]
[1]Ryerson University, Toronto, Canada

ABSTRACT

The use of Model Predictive Controllers (MPC) in building HVAC systems has demonstrated significant energy savings. This approach relies on knowledge of occupancy, weather conditions, and building thermal dynamics to predict the future HVAC conditioning requirements. The thermal dynamics is usually modeled using a grey box model, which requires the knowledge of the buildings thermal mass, an unknown characteristic for many older buildings. This study analyzes the ability to determine thermal dynamic behavior without building construction knowledge. A test cell has been constructed to monitor typical building control points consisting of the ambient temperature, supply air conditions, occupancy, lighting, and plug loads along with outdoor air temperature and solar radiation. These are used in conjunction with surface temperature sensors to characterize their thermal response with the outdoor and indoor conditions. This paper presents the set-up of the test cell along with the preliminary study investigating the ability to solve for thermal mass using sensor measurements. The analysis conducted looks at the simplest thermal condition of the cell, the nighttime unoccupied condition, for the two most thermally slow elements, the concrete floor and ceiling slabs. The results from this preliminary analysis strongly indicate the potential to calculate thermal dynamic behavior using only BAS points. This will support the overall research goal of creating model predictive control approaches for existing building where exact thermal mass is unknown.

INTRODUCTION

The building sector is estimated to consume 40 percent of the world's energy and generate 33 percent of carbon dioxide emissions (Huang, *et al.*, 2015a). Within building energy use almost half is used towards heating, ventilation, and air conditioning (HVAC). The most common type of HVAC control system is the proportional-integral-derivative control (PID) system or On-Off method. To reduce the amount of emissions generated from HVAC systems, research has started to look into smarter control systems such as Model Predictive Control (MPC). Studies conducted on MPCs have demonstrated significant energy savings compared to typical HVAC control, for example (Dong & Lam, 2014; Huang, *et al.*, 2015a).

MPCs use an HVAC control algorithm with inputs of predicted weather and occupancy along with the buildings thermal dynamics. This control system is more efficient than PID control because it is both a predictive and reactive system. MPCs are able to significantly reduce energy consumption because it incorporates knowledge of the buildings thermal response. This information allows the control system to avoid over-cooling or over-heating, a common issue for traditional (reactive) control systems such as PID and On-Off control methods (Huang, *et al.*, 2015b).

Three types of building models may be used to support MPC: *white box*, *black box* or *grey box*. White box refers to purely analytical models. These models rely on detailed physics equations to precisely capture the behavior of the building. Such models are time-consuming to create and solve, and requires a comprehensive knowledge of building characteristics (Li & Wen, 2014). Many studies use computational energy simulation programs such as *EnergyPlus* (Ma, *et al.*, 2012) to create these white box models.

Opposite to white-box models, black-box models incorporate no mathematical descriptions of actual physical processes. Black-box models instead use input data and machine learning techniques to predict the building behavior. These models have been shown to use a range of prediction algorithms varying from regression models (Mustafaraj, *et al.*, 2011), to more sophisticated algorithms such as Artificial Neural

Networks (Huang, *et al.*, 2013), Genetic Algorithms, and Fuzzy Logic (Afram & Janabi-Sharifi, 2014). This style of data driven thermal dynamic modeling puts emphasis on the quality and quantity of data collected as there is a high risk of skewing the forecast model based on the data used (Li & Wen, 2014).

A grey box model is a hybrid of the white and black box models, combining a simplified analytical model with input data to create a predictive model. This method has been shown to be the most effective technique for use of predictive building operations (Amara, *et al.*, 2015). The simplified physical model most commonly used within grey box models are R-C networks, for example (Dong & Lam, 2014). R-C networks are preferred due to their ability to represent physical behavior while maintaining computation efficiency as shown in (Huang, *et al.*, 2015a). Harb *et al.* (2016) determined that the most accurate RC network structure for the use of grey box models is a 4R2C network.

As with white box models, the difficulty with grey box models is the need for the buildings construction details. Many older buildings, where MPC could offer significant benefit, there is minimal as-built information. Recent research has aimed to address this issue, for example Carrascal *et al.* (2016) used statistical techniques to estimate the unknown building element resistances and capacitances in order to implement MPC, resulting in 10-15% energy savings.

Given the significant fraction of the built environment where limited as-built information has historically precluded MPC implementation, research is underway to develop an alternative approach that leverages commonly available data from Building Automation Systems (BAS) to implement MPC. If successful, this approach will substantially broaden the applicability of MPCs within aging buildings. This paper presents the implementation of a test cell to support this research along with preliminary data findings for the simplest condition, namely unoccupied nighttime conditions. These findings will support the expansion of the model to a broader – and thus more generalizable – set of conditions.

METHODOLOGY

This study uses an office space within a 1970-era University building (concrete construction; Brutalist architectural style) as the test cell. The cell is set up with a variety of sensors, summarized in Table 1, to track the energy loads and behaviors of the space. The following section describes the physical characteristics of the cell, the types of data sensors installed within the space, and their calibration.

Test cell design and calibration

The test cell is approximately 8.4m^2 featuring one east-facing external wall with three window panes and one spandrel panel. The windows are double pane aluminum frame, and the spandrel panel is made of steel sheets sandwiching rigid insulation. The floor/ceilings and exterior siding is constructed of thick concrete slabs with the interior walls constructed of gypsum board and steel

Table 1 Test cell sensors

DATA COLLECTED	SENSOR (MAKE AND MODEL)	DESCRIPTION
Surface Temperature	MadgeTech OctTemp with Type T Thermocouples	Temperature [0.1°C resolution, +/- 0.05°C accuracy] of each surface within the test space
Ambient Temperature	*OmniSense S-10* Ambient Sensors	Temperature [+/- 0.4°C accuracy] and relative humidity of ambient air at four locations around the test space.
Solar Radiation	0.5V, 100mA PV Panel	PV panel is mounted on the glazing facing outwards and the irradiance measurement [0.1W/m^2 resolution, +/- 10W/m^2 accuracy] is calculated based on output voltage.
Ventilation Input	*Modern Devices* Wind Sensor Rev P	The unit reads the temperature and flow rate of the incoming air from the ventilation ducts and transmits the data to the Arduino.
Electrical Watts	Watts up? PRO	A Wattmeter measures power consumption +/-0.1W at the power bar serving the computer and other electrical equipment.
Occupancy	Toggle switch	Manual toggle switches are used by people entering the test cell to record occupancy data on the Arduino.
Interior Lighting	Toggle switch	A manual toggle switch next to the light switches of the lab sends ON/OFF status to the Arduino.
Door Position	Reed switch	A reed switch is set up on the door of the office to record its OPEN/CLOSED position on the Arduino.

framing. A 3D view of the test cell indicating sensor position is shown in Figure 1; note that hollow rectangles represent the sensors on the opposite side of the wall.

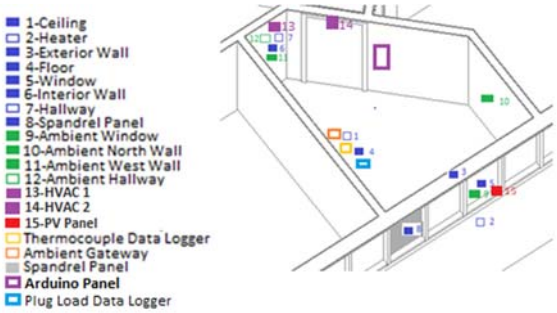

Figure 1 Test cell layout

The rooms surrounding the test cell are all conditioned by the same HVAC (water source heat pump) unit, with exception to the rooms above and below the cell. There is minimal time where the cell experiences direct sunlight due to the eastern orientation and proximity to other surrounding buildings.

The surface temperature of various locations within the test lab is being read by a MadgeTech OctTemp data logger using Type T (copper/constantan) thermocouples, which are attached with thermally conductive paste to eight surfaces, as seen in Figure 1. Each temperature is read and recorded by the OctTemp data logger, which was placed in the center of the room to equalize the length of the thermocouple wiring so that discrepancies in the data due to resistance losses are minimized. Each thermocouple was calibrated using both an ice bath and boiling water. The surface temperature readings will be used for model training, testing/tuning, and validation.

The ambient temperatures within the cell are recorded using *OmniSense S-10* wireless temperature sensors that connect to the *OmniSense* gateway. These sensors give information about the ambient air temperature and relative humidity at four locations around the cell. These sensors are manufacturer-calibrated with a lifetime guarantee and were not recalibrated.

The *Arduino Mega* unit in the test cell collects data for solar radiation, ventilation input, occupancy, interior lighting, and door position. The *Arduino Mega* is connected to an SD Card breakout board and a *Real Time Clock* unit, which timestamps the data as it is written. The SD Card is manually transferred to a laptop weekly.

To provide better granularity than an occupancy sensor (which does not indicate the number of occupants), four switches were installed at the entrance to the room to be turned on by individuals as they enter and turned off as they leave, with each additional person indicating their presence with the subsequent switch. Each switch is numbered and an LED associated with each switch provides a visual confirmation of the count to minimize error while the Arduino records the highest switch in the ON positon.

The interior lights are also recorded using a manual switch connected to the Arduino. The lights OFF position is indicated as '0' and ON as '1'. The switch is located directly next to the light switches for the cell to permit the user to turn on all switches with a single movement.

The door position status is documented using a reed switch connected to the Arduino. The switch opens and closes the circuit using a magnetic field. A magnet is attached to the door such that it provides this field when the door is in the fully closed position. Note that the degree of door openness cannot be measured with this set-up and thus the occupant was requested to ensure that the door is either fully open or fully closed.

The test cell experiences little direct sunlight therefore a simple pyranometer consisting of a small (0.5V, 100mA) photovoltaic panel is used to capture solar gains. The pyranometer circuit diagram allowing the current to be determined based on output voltage is illustrated in Figure 2.

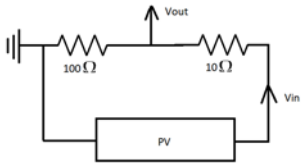

Figure 2 Pyranometer circuit

The *Arduino Mega* reads this voltage at an analog input pin and calculates the solar gains using a correlation developed using irradiance meter measurements taken over several days for calibration.

Supply airflow rate and temperature are measured by the *Modern Device* Wind Sensor Rev P probe. The output voltage of this probe (V_{probe}) is read by the Arduino, which converts this reading into temperature (°C) and velocity (v in m/s) using Eq. 1 and 2. Note that the 0.447 term within the velocity equation is the conversion factor from miles per hour (manufacturer-supplied code) to meters per second (desired units).

$$T_{vent} = \frac{\left(\left(\frac{(V_{probe} * 5)}{1024}\right) - 0.4\right)}{0.0195} \quad (1)$$

$$v_{vent} = \left[\frac{(V_{probe} - 264)}{85.68}\right]^{3.37} * 0.447 \quad (2)$$

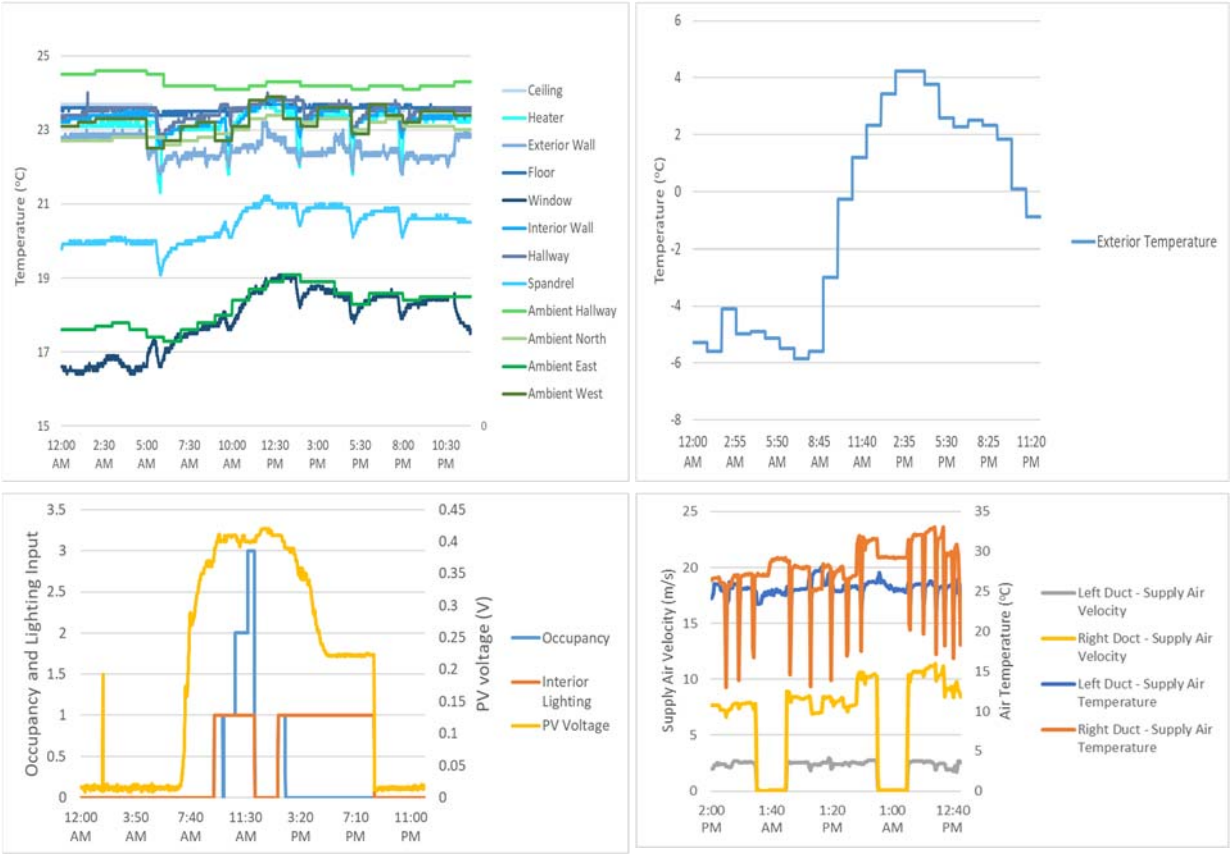

Figure 3 Sample data points from the test cell (November 23, 2017)

The Wind Sensor Rev P temperature sensors were calibrated to within ±1.0ºC and ±1.5 ºC for the right and left ducts using a Temperature-RH probe. The airflow measurements were calibrated using a balometer, achieving calibration to within ±2CFM with variations up to ±6CFM for both ducts. The PV panel irradiance measurements are calibrated to within ±10W/m^2.

Data correlation

Full data collection from the three sensor loggers began at the beginning of November 2017. Figure 3Figure 3 illustrates the sensor readings on a typical weekday in November. The first graph demonstrates the surface and ambient temperature readings. The second graph demonstrates the outdoor air temperature readings. The third graph demonstrates the data collected from the *Arduino* unit including the occupancy, lighting and solar sensors. The final graph shows the supply air velocity and temperature for both the ventilation ducts.

RESULTS

The data collected in the early heating season (December through January) were analyzed to evaluate data quality obtained by the test cell. A preliminary regression analysis conducted during the simplest condition (nighttime, unoccupied, ventilation off) was undertaken to determine whether floor and ceiling slab temperatures could be determined from the other variables measured. This paper presents the findings from the preliminary analysis and discusses the insights gained applicable to the overall research goal - creating a grey-box model which can infer building thermal dynamics using BAS points.

Observed variable relationships

Preliminary relationships between data points were observed from daily and weekly data plots as follows:

1. The window surface temperature is the lowest of all thermocouple measurement and follows the exterior weather temperature, as expected. All of the temperature sensors are seen to have greater variance during the day when the test cell is experiencing a larger variance in energy loads and a steadier temperature measurement at night. Of all of the eight surfaces within the test space, the most consistent temperature is seen in the ceiling and the floor slabs as they have the greatest thermal mass,

and varied by less than 0.1°C (the sensor resolution) over the 12am-5am period of each day.

2. The ambient temperature sensors demonstrate a level of horizontal stratification along the cell. The easternmost sensor, which is adjacent to the window, has the lowest temperature readings. Ambient temperatures increase through the center of the cell, and the highest temperatures are measured in the hallway outside the cell. The ambient sensor at the west side of the cell approximately 1m below the ventilation ducts is the most sensitive to supply air effects, indicating limited supply air mixing across the cell.
3. The ventilation schedule for the cell was observed in both the ambient sensor data and the airflow measurement data. The ambient temperature sensor below the ventilation ducts demonstrates very little variation between the hours of 12:00am to 5:00am. The duct velocity sensors indicate near-zero airflow readings between these hours, most likely due to natural convection in the room. Based on the daily repetition of this pattern, it is evident that the HVAC unit is scheduled off during this period. Analyzing daily temperatures, it is clear that a 7-day schedule is used, with the weekend days showing the same performance as nighttime days. A short HVAC shutdown from December 30-January 1, providing an opportunity for isolating solar gain effects.

This analysis also revealed an issue with the preliminary installation of the solar cell. As evident from Figure 3, the solar readings step up and down at the same time as the interior lighting, indicating that it was reading artificial lighting as solar gain. Based on this observation, the PV was relocated (mounted on the glazed surface). The data collected during this period requires adjustment to both remove the internal light effects and recalibrate for the new photovoltaic cell orientation. A minor issue was also noticed pertaining to short trips into or out of the office where the occupant frequently neglected to change the occupancy switch position, resulting in a slight under- or over-estimation of occupancy for brief periods.

Data selection

The simplest analysis to consider is the unoccupied nighttime condition (12:00am to 5:00am) for the two highest thermal mass elements: the ceiling and the floor slabs. The energy loads affecting the temperature of these slabs during the nighttime period is the ambient temperature (T_{amb}), the exterior weather conditions (ΔT_{Ext}), the heat generated from the plug loads (W_{pl}), the heat from the radiant heater (T_{heat}), the temperature of the hallway (ΔT_{Hall}) as well as each of the slab temperatures (T_{ceil}, T_{floor}). The temperature gradient across the exterior wall and interior wall was determined using the exterior and hallway temperatures. These values are used within the regression models to represent the degree of heat loss/gain.

The data was plotted to see any obvious trends or abnormalities. An unusual spike in the floor temperature was observed from December 16th-18th, shown in Figure 4. Preliminary linear trend analysis demonstrated that the spike had a significant impact on the data correlation. As the spike is an unexplainable abnormality, it was decided for this study to omit this data.

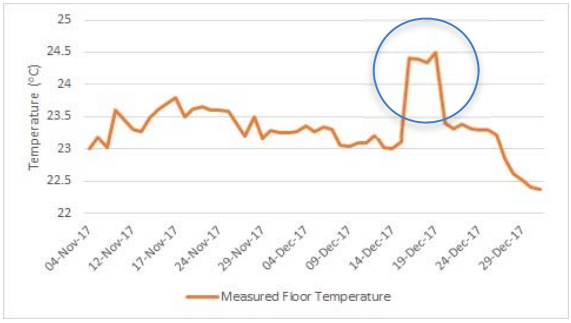

Figure 4 Floor slab temperature

Regression analysis and hypothesis testing

Multiple linear regression analysis was undertaken to identify the optimal combination of dependent variables. An additive regression approach was applied to training data (80% of complete data set) collected in December through mid-January. The regression model results were analyzed based on their Root Mean Square Error (RMSE) and p-value based on the student t-test. The null hypothesis for every regression analysis was all dependent variables having a coefficient, β_n, equal to zero.

$$H_0: \quad \beta_n = 0 \tag{3}$$

$$H_1: \quad \beta_n \neq 0 \tag{4}$$

For each iteration of the additive regression analysis the best regression model is chosen based on the smallest RMSE. The p-value results demonstrate whether or not each variable rejects the null hypothesis at 90%, 95% and 99% confidence intervals.

Table 2 t-values for respective confidence intervals

CONFIDENCE INTERVALS	P-VALUE	CRITICAL T-VALUE (N>>10,000)
95%	0.05	1.960
99%	0.01	2.576
99.9%	0.001	3.291

The additive linear regression starts by modeling the surface temperature against each of the energy loads. The model which has the best fit defined by the lowest RMSE, is carried onto the second regression whereby each of the remaining energy loads is individually added to the first regression model and tested to determine whether the RMSE improves significantly (i.e. P<0.05) observed for lower RMSE results. This process is repeated for subsequent iterations until the addition of new variables ceases to improve the prediction results significantly. The order of the variables in represents the order of addition to the model. This approach minimizes the computational cost of the final model while maintaining accuracy. The full additive regression models, using all six variables, are shown in Eq. 5 and Eq. 6. The p-values for each model is shown in Tables 3 and 4. The corresponding RMSE values for these two models are 0.169 and 0.0827, which both fall between the measurement precision of the thermocouples:

$$T_{s\_ceiling} = 0.94 + 0.44T_{amb} + 0.57T_{Floor} - 0.01W_{pl} - 0.01T_{Heat} + 0.04\Delta T_{Hall} - 0.001\Delta T_{Ext} \quad (5)$$

$$T_{s\_floor} = 0.92 + 0.83T_{amb} + 0.32\Delta T_{Hall} + 0.008\Delta T_{Ext} + 0.15T_{ceiling} - 0.007T_{Heat} + 0.0002W_{pl} \quad (6)$$

Table 3 Calculated p-values for the full additive ceiling regression model

P-VALUE					
$p(T_{amb})$	$p(T_{Floor})$	$p(W_{pl})$	$p(T_{Heat}$	$p(\Delta T_{Hall})$	$p(\Delta T_{Ext}$
1.13E-07	<2E-16	<2E-16	<2E-16	5.94E-06	0.108

Table 4 Calculated p-values for the full additive floor regression model

P-VALUE					
$p(T_{amb})$	$p(\Delta T_{Hall})$	$p(\Delta T_{Ext})$	$p(T_{ceiling})$	$p(T_{Heat})$	$p(W_{pl})$
<2E-16	<2E-16	<2E-16	<2E-16	<2E-16	0.506

The results from the full ceiling regression model, shown in Table 3, demonstrated a high p-value for the sixth variable (ΔT_{Ext}). This variable does not reject the null hypothesis for any confidence interval and is eliminated from the model. The model therefore returns to the previous five variable model which, has equal RMSE value to the four-variable model. As the addition of the fifth variable did not improve the fit of the model it can be omitted and the previous four variable model is used as the best fit for the ceiling slab. This model is demonstrated in Eq. 7 with RMSE value of 0.169. The p-values are shown in Table 5, with all variables significant above a 99% level, thus rejecting the null-hypothesis.

$$T_{s\_ceiling} = 1.28 + 0.36T_{amb} + 0.63T_{Floor} - 0.01W_{pl} - 0.02T_{Heat} \quad (7)$$

Table 5 Final regression analysis calculated p-values for the ceiling slab temperature

P-VALUE			
$p(T_{amb})$	$p(T_{Floor})$	$p(W_{pl})$	$p(T_{Heat})$
<2E-16	<2E-16	<2E-16	<2E-16

The floor slab full additive regression model results, are similar to the ceiling slab. The sixth variable, W_{pl}, resulted in a p-value that did not reject the null hypothesis for any confidence interval, eliminating the variable from the model. The previous five variable model has the lowest RMSE value and is therefore the best fit model for the floor slab. The final floor model is shown in Eq.8, with RMSE value of 0.0827. The p-values are shown in Table 6, with all variables significant above a 99% level, thus rejecting the null-hypothesis.

$$T_{s\_floor} = 0.94 + 0.83T_{amb} + 0.32\Delta T_{Hall} + 0.008\Delta T_{Ext} + 0.15T_{ceiling} - 0.007T_{Heat} \quad (8)$$

Table 6 Final floor regression model calculated p-values for the floor slab temperature

P-VALUE				
$p(T_{amb})$	$p(\Delta T_{Hall})$	$p(\Delta T_{Ext})$	$p(T_{ceiling})$	$p(T_{Heat})$
< 2E-16	< 2E-16	< 2E-16	< 2E-16	< 2E-16

Using the temperature equations from the final regression models above, the predicted ceiling and floor temperatures were calculated using the testing data (20% of complete data set). Plots of the predicted vs. measured temperatures for the floor and ceiling slabs, respectively are shown in Figures 5 and 6. In both cases, the temperatures predicted using the regression equations have good agreement with the measured data. These results support the ability for the test cell's thermal behavior to be determined using data commonly collected from BAS points. By extension, this demonstrates the potential in future research to support model predictive control in more complex conditions such as occupied hours with HVAC, incident solar

radiation, and highly variable plug loads. This will be further beneficial since the slab temperatures can be defined as a combination of known or target (i.e. future ambient temperature) variables.

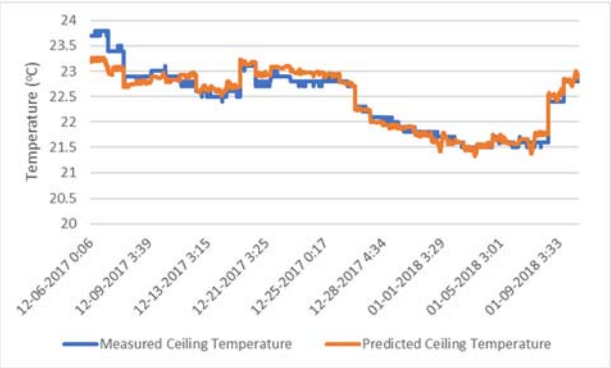

Figure 5 Predicted vs. measured ceiling temperature

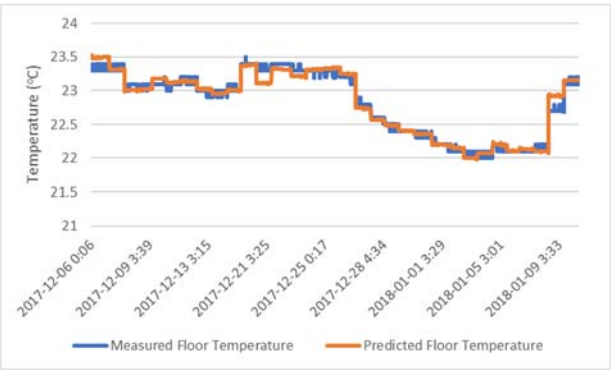

Figure 6 Predicted vs. measured floor temperature

CONCLUSIONS

The purpose of this study was to design a test cell for use in investigating the potential to infer thermal dynamics using BAS data points. The test cell was successfully set up and calibrated with eight different sensor types. It is steadily collecting both the input data for the model (lighting, occupancy, solar gain, ventilation input, ambient temperature and plug load) and the training data (surface temperatures).

The regression analysis conducted for the ceiling and floor slab found that during the simplest test condition both surface temperatures have good correlation to the energy loads in the environment. These models demonstrated the ability to predict the ceiling and floor surface temperatures with use of BAS points. The results support the potential with the use of more sophisticated algorithms, such as artificial neural networks and/or fuzzy algorithms, to expand the predictions to complete cell behavior including future ambient conditions. Overall, this paper's findings support the larger research goal of investigating the ability to determine thermal dynamics without building construction knowledge.

Error discussion

The test cell data is affected by three main sources of error: (1) generalization of point measurements, (2) sensor resolution and accuracy, (3) human behavior.

The solar gain, ventilation temperature/airflow and surface temperature data are point measurements that are assumed to be uniform across the entire measurement area. To minimize the error arising from the generalization of point measurements, wherever possible, these sensors are compared to other spot measurements or, in the case of duct velocity where a balometer could be used to measure total flow rates, true measurements. Ambient temperatures were taken in the occupied zone as is typical of BAS devices, which is what this test cell is mimicking. Because the models typically used in MPC assume 1-d heat transfer from representative nodes, the thermocouples within the cell were installed at the center of each building element to avoid edge conditions, which are not picked up in the analytical model being developed. Because of the nature of the model (1-d using representative nodes) and the end goal of the research, these simplifications are acceptable.

Measurement error is minimized by calibrating each of these sensors against a device with known calibration: PV against a factory calibrated illuminance meter, velocity sensor against a balometer, and temperature/RH sensors against a temperature/RH probe. Further, all thermocouples were tested using a standard boiling water bath and ice bath alongside a verified thermometer. The boiling and ice water bath calibration measurements were input to the Madgetech data logging software for automatic calibration with an input offset of ±0.5°C. Ambient sensors are factory-calibrated with a lifetime guarantee of accuracy within ±0.4°C. Because this paper addresses the simplest case, these surface and ambient temperature measurements are the only potential error sources, however for future research an evaluation of other potential measurement error and ongoing calibration are critical to ensure a robust data set. Using Eq. 9 for a function based on n inputs and applying this to the final regression equations, the expected impact of measurement error on ceiling slab prediction is ±0.3465°C, which is twice the calculated RMSE and on a similar order of magnitude to the precision of the thermocouple. The floor slab prediction has an estimated measurement error of ±0.3855°C, which is again similar to the precision of the surface temperature sensor, but much higher than the prediction RMSE.

$$e_{measurement} = \sqrt{\sum_{i=1}^{n}\left[\partial x_i{}^2 * \left(\frac{\partial F}{\partial x_i}\right)^2\right]} \qquad (9)$$

The manual occupancy and interior lighting toggle switch measurements collected from the test cell are subject to human error. Although it does not impact the model for the simplest case study, it is an item requiring resolution for occupied cases. For the early data collected, this error can be minimized by cross examining the occupancy data against the lighting status, the door position and plug load data. The data within the time period of this study was analyzed and determined that twice out of twelve occupancy periods were not recorded by the user but was fixed by cross examining the other data points mentioned. Similarly, the door position is an operator dependent measurement. The door is measured in either an "OPEN" or "CLOSED" position with the sensor unable to tell the degree in which the door is open. The operator is asked to keep the door in either the fully open or fully closed position so that the data can be analyzed as "OPEN" having full air exchange with the hallway or as "CLOSED" having minimal exchange. During situations when the operator leaves the door in a partially opened position the state of the cell will still be analyzed with complete air exchange. This is being resolved through the installation of a pair of laser sensors that detect motion into and out of the test cell based on the occupants passing two parallel laser paths.

Future research

This preliminary study has indicated strong potential for the inference of thermal dynamics in building elements due to BAS data. The next stage of research will develop an Adaptive Fuzzy Inference System (ANFIS) for this simplified case and expand it with progressively more input variables. A white box model is also under development and the ANFIS-developed coefficients will be introduced into this white box model to refine the predictive model.

ACKNOWLEDGMENT

The authors gratefully acknowledge the financial assistance received from the Ontario Research Fund – Research Excellence (ORF-FE) Big Data Research Analytics Information Network (BRAIN) Alliance and FuseForward solutions to support this project.

REFERENCES

Afram, A. & Janabi-Sharifi, F., 2014. Theory and applications of HVAC control systems–A review of model predictive control (MPC). *Building and Environment,* Volume 72, pp. 343-355.

Amara, F. et al., 2015. Comparison and Simulation of Building Thermal Models for Effective Energy Management. *Smart Grid and Renewable Energy,* pp. 95-112.

Carrascal, E., Garrido, I., Garrido, A. J. & Sala, J. M., 2016. Optimization of the Heating System Used in Aged Buildings Via Model Predictive Control. *Energies.*

Dong, B. & Lam, K., 2014. A real-time model predictive control for building heating and cooling systems based on the occupancy behavior pattern detection and local weather forecasting. *Building Simulation,* 7(1), pp. 89-106.

Harb, H. et al., 2016. Development and validation of grey-box models for forecasting the thermal responce of occupied buildings. *Energy and Buildings,* pp. 199-207.

Huang, H., Chen, L., Hu & E., 2015b. A neural network-based multi-zone modelling approach for predictive control system design in commercial buildings. *Energy and Buildings,* Volume 97, pp. 86-97.

Huang, H., Chen, L. & Hu, E., 2015. A new model predictive control scheme for energy and cost savings in commercial buildings: An aairport terminal building case study. *Building and Environment,* pp. 203-216.

Huang, H., Chen, L., Hu & Eric, 2015a. A new model predictive control scheme for energy and cost savings in commercial buildings: An airport terminal building case study. *Building and Environment,* Volume 89, pp. 203-216.

Huang, H. et al., 2013. *Multi-zone temperature prediction in a commercial building using artificial neural network model,* Hangzhou, China: 10th IEEE International Conference on Control and Automation (ICCA).

Li, X. & Wen, J., 2014. Review of building energy modeling for control and operation. *Renewable and Sustainable Energy Reviews,* pp. 517-537.

Ma, J., Qin, J., Salsbury, T. & Xu, P., 2012. Demand reduction in building energy systems based on economic model predictive control. *Chemical Engineering Science,* pp. 92-100.

Mustafaraj, G., Lowry, G. & J.Chen, 2011. Prediction of room temperature and relative humidity by autoregressive linear and nonlinear neural network models for an open office. *Energy and Buildings,* pp. 1452-1460.